AIAA JOURNAL
Vol. 30, No. 12, December 1992

Active, Passive, and Semiactive Vibration Suppression by Stiffness Variation

Junjiro Onoda*
Institute of Space and Astronautical Science, Kanagawa 229, Japan
Tetsuji Sano†
University of Tokyo, Tokyo 111, Japan
and
Kohichi Kamiyama‡
Nihon University, Chiba 275, Japan

This paper investigates the vibration suppression by stiffness variation. First, optimal on-off control logic for a single-degree-of-freedom variable-stiffness system is proposed. A control logic for a multiple-degree-of-freedom system with multiple variable-stiffness elements is also proposed. As an example of a variable-stiffness system, a string whose tension is controllable is studied. Numerical simulation demonstrates the effectiveness of the proposed control logic. Next, a dry friction is shown to vary the tension of a string in the same way as this active control when the longitudinal stiffness is high, realizing a passive vibration suppression. The performance of the passive system is studied. To overcome the disadvantages of the passive system, a semiactive control is proposed, that controls the frictional force. Numerical simulations and an experiment demonstrate its effectiveness and robustness, although it is primitive.

Introduction

LARGE space structures are expected to be flexible because of the stringent demands of lightweight and large dimensional size. Their damping is also expected to be very slow, whereas the shape accuracy requirements are stringent in many future missions, including the huge space antennas and optical interferometers. Therefore, the vibration suppression of space structures is an important and difficult problem.

One of the most attractive approaches for this problem is active vibration suppression.[1] Numerous works have been reported about this subject. In most of them, the control forces or torque are directly applied to the structure to suppress the vibration. However, in some of them, another approach, the vibration suppression by stiffness variation, is studied. To suppress the lateral vibration of tension-stabilized strings, Chen[2] has proposed to control their tension. Because the lateral stiffness of the string is proportional to its tensile force, his work suggests that the vibration can be suppressed by varying the stiffness. Later, Fanson et al.[3] and Sekine[4] studied the vibration suppression by this type of stiffness variation. Recently, Onoda et al.[5] introduced another type of hysteretic variable-stiffness system, which is referred to as type II, whereas the known variable-stiffness system such as variable-tension strings is called type I in theor paper. They showed a significant difference between the characteristics of the two types, especially that the type II variable-stiffness system is always stable even if it is improperly controlled. Furthermore, they proposed an approach to suppress the vibration of multiple-degrees-of-freedom (MDOF) systems by controlling the stiffness of type II variable-stiffness elements. However, the general strategy for the vibration suppression of MDOF vibration of the type I system by the stiffness control does not seem to have been studied sufficiently.

The active vibration suppression is usually very powerful. However, the spillover instability is still a tough problem in the active vibration suppression, even though many works have been published on robust control logic. On the other hand, passive systems, which have no artificial control and whose vibration energy is dissipated by the structural damping, viscosity, friction, etc., are always stable. This robustness is their great advantage. Therefore, it seems to be meaningful to investigate if the vibration can be suppressed by the stiffness variation resulting from passive devices. In many cases, however, passive systems have disadvantages in their performance. A possible attractive approach to reduce this disadvantage, keeping the advantages of passive systems, may be the semiactive vibration suppression, which controls the states of the systems such that the damping performances are maximized.

In this paper, the investigation concentrates on type I variable-stiffness systems. First, active vibration suppression of single and multimode vibrations of a type I variable-stiffness system is studied and a control logic is proposed. Next, it is applied to the active vibration suppression of a string, which is a typical example of a type I variable-stiffness system (and also the simplest example of tension-stabilized structures), and modified into a more suitable form for the local implementation. Subsequently, it is shown that the stiffness variation that is equivalent to this active control can be implemented by using passive dry friction if the longitudinal stiffness of the string is high. This system with dry friction is robust because it is a passive system. But if the longitudinal stiffness is not high enough, vibration ceases to be suppressed when it has been suppressed to a certain level because the frictional slip stops. As a result, a certain amplitude of residual vibration remains. Therefore, a semiactive approach is proposed to eliminate the disadvantages, including the residual vibration, still keeping the advantage of robustness. The effectiveness of these approaches is investigated and compared with each other other based on the numerical simulations. Finally, an experi-

Received Feb. 13, 1992; presented as Paper 92-2090 at the AIAA Dynamics Specialists Conference, Dallas, TX, April 16-17, 1992; revision received May 14, 1992; accepted for publication May 15, 1992.

*Professor, Research Division of Space Transportation, 3-1-1, Yoshinodai, Sagamihara-shi. Member AIAA.

†Graduate Student, Department of Aeronautics, Faculty of Engineering, 7-3-1, Hongo, Bunkyo-ku.

‡Graduate Student, Department of Mechanical Engineering, College of Industrial Technology, 1-2-1, Izumi-cho, Narashino-shi.

ment is performed to demonstrate the effectiveness and practicality of semiactive vibration suppression.

Active Vibration Suppression of a Single-Degree-of-Freedom System

When the external force is zero, the equation of motion of a single-degree-of-freedom (SDOF) type I variable-stiffness system is

$$m\ddot{u} + \tilde{k}u = 0 \tag{1}$$

where m is the mass, $\tilde{k}$ the variable stiffness, and u the displacement. Usually, the variation range of stiffness $\tilde{k}$ is limited by the hardware capability. Therefore, let us assume as

$$k(1-\epsilon) \le \tilde{k} \le k(1+\epsilon) \tag{2}$$

where k is the nominal stiffness and ϵ is a constant. Then the vibration is most reduced per cycle by controlling the stiffness such that[5]

$$\tilde{k} = \begin{cases} k(1+\epsilon) & \text{if } u\dot{u} > 0 \\ k(1-\epsilon) & \text{if } u\dot{u} < 0 \end{cases} \tag{3}$$

However, it should be noted that this control logic does not necessarily result in the maximum damping per time, which is our goal.

To obtain the on-off control logic which damps the vibration most rapidly, let us modify the control logic of Eq. (3) as follows:

$$\tilde{k} = \begin{cases} k(1+\epsilon) & \text{if } (u-\gamma_1\xi)(\xi+\gamma_2 u) > 0 \\ k(1-\epsilon) & \text{if } (u-\gamma_1\xi)(\xi+\gamma_2 u) < 0 \end{cases} \tag{4}$$

where

$$\xi \equiv \sqrt{m/k}\,\dot{u} \tag{5}$$

and where γ_1 and γ_2 are constants related to the on-off timing. Then it can be seen from Eqs. (1) and (4) that the amplitude of vibration decreases by the factor of

$$r_h = \frac{(1-\epsilon+\gamma_2^2)[1+\gamma_1^2(1+\epsilon)]}{(1+\epsilon+\gamma_2^2)[1+\gamma_1^2(1-\epsilon)]} \tag{6}$$

per half-cycle, and the half-cycle period T_h is

$$T_h = \frac{1}{\omega}\left\{\frac{1}{\sqrt{1+\epsilon}}\tan^{-1}\frac{(1+\gamma_1\gamma_2)\sqrt{1+\epsilon}}{[\gamma_1(1+\epsilon)-\gamma_2]} + \frac{1}{\sqrt{1-\epsilon}}\tan^{-1}\frac{(1+\gamma_1\gamma_2)\sqrt{1-\epsilon}}{[\gamma_2-\gamma_1(1-\epsilon)]}\right\} \tag{7}$$

where

$$\omega = \sqrt{k/m} \tag{8}$$

By using these equations, the optimal values of γ_1 and γ_2 that maximize the equivalent damping ratio

$$\zeta \equiv -1/(T_h\omega)\,\ln(r_h) \tag{9}$$

are numerically searched. The optimal values of γ_1 and γ_2, the resulting optimal damping ratio, and the damping ratio resulting from other types of control logic, including Eq. (3) (i.e., $\gamma_1 = \gamma_2 = 0$), are shown in Fig. 1 against ϵ. The figure shows that the optimal timing of stiffness reduction is later than the control logic of Eq. (3), whereas that of stiffness recovery is the same as it. The optimal value of γ_2 coincides with the optimal damping ratio. The figure shows the advantage of the control logic of Eq. (4) over the logic of Eq. (3) when ϵ is relatively large. This advantage is brought in by the reduction of the cycle period due to the delay of the stiffness reduction timing. For the logic of Eq. (3), ϵ has an optimal value, that is slightly less than 0.9. Beyond this value, the damping ratio decreases because the cycle period becomes longer.

When the stepwise variation of stiffness is not practical, the following logic can be used instead of Eq. (4):

$$\tilde{k} = \begin{cases} k(1+\epsilon) & \text{if } \alpha(u-\gamma_1\xi)(\xi+\gamma_2 u) \ge \epsilon \\ k[1+\alpha(u-\gamma_1\xi)(\xi+\gamma_2 u)] & \text{if } -\epsilon < \alpha(u-\gamma_1\xi)(\xi+\gamma_2 u) < \epsilon \\ k(1-\epsilon) & \text{if } \alpha(u-\gamma_1\xi)(\xi+\gamma_2 u) \le -\epsilon \end{cases} \tag{4'}$$

where α is a constant.

In Ref. 2, the following two types of control logic are shown to be effective;

$$\tilde{k} = \begin{cases} k(1+\alpha_1\dot{u}) & \text{if } u > 0 \\ k(1-\alpha_1\dot{u}) & \text{if } u < 0 \end{cases} \tag{10}$$

$$\tilde{k} = \begin{cases} k(1+\alpha_2 u) & \text{if } \dot{u} > 0 \\ k(1-\alpha_2 u) & \text{if } \dot{u} < 0 \end{cases} \tag{11}$$

The damping ratio obtained by these two types of logic are also calculated and plotted in Fig. 1. The gain constants α_1 and α_2 are adjusted such that

$$\epsilon = \alpha_1 |\dot{u}|_{\max} \tag{12}$$

$$\epsilon = \alpha_2 |u|_{\max} \tag{13}$$

so that the stiffness variation does not exceed the limit of Eq. (2), where $|\dot{u}|_{\max}$ and $|u|_{\max}$ are the maximum values of $|\dot{u}|$ and $|u|$ in a cycle of vibration, respectively. The figure shows much rapid damping of the on-off control compared with those of Eqs. (10) and (11); even the control logic of Eq. (3) results in a superior damping.

Active Vibration Suppression of an MDOF System with Multiple Variable-Stiffness Members

When the external force is zero, the equation of motion of an MDOF system is

$$\boldsymbol{M}\ddot{\boldsymbol{u}} + \tilde{\boldsymbol{K}}\boldsymbol{u} = 0 \tag{14}$$

where $\boldsymbol{M}$ is the mass matrix, $\tilde{\boldsymbol{K}}$ the variable stiffness matrix, and $\boldsymbol{u}$ the displacement vector. Let us assume that the variable-stiffness matrix $\tilde{\boldsymbol{K}}$ is a linear function of drive signals s_j to the jth variable-stiffness structural element as

$$\tilde{\boldsymbol{K}} = \boldsymbol{K} + \sum_{j=1}^{nv} s_j \Delta\boldsymbol{K}_j \tag{15}$$

where $\boldsymbol{K}$ is the nominal stiffness matrix, $\Delta\boldsymbol{K}_j$ is the variation of stiffness matrix due to the unit drive signal to the jth variable

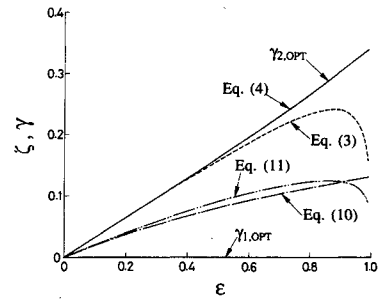

Fig. 1 Equivalent damping ratios of an actively controlled SDOF system and the optimal values of γ_1 and γ_2.

stiffness element, n_v is the number of variable stiffness elements, and the range of s_j is limited to

$$-1 \le s_j \le 1 \tag{16}$$

In the modal coordinates based on the mode shapes of the structure whose stiffness is $\boldsymbol{K}$, the equation of motion is as follows:

$$\ddot{\boldsymbol{q}} + (\Omega + \boldsymbol{G})\boldsymbol{q} = 0 \tag{17}$$

where

$$\boldsymbol{G} \equiv \sum_{j=1}^{n_v} s_j \Phi^T \Delta \boldsymbol{K}_j \Phi / m \tag{18}$$

$$\Omega \equiv \mathrm{diag}(\omega_1^2, \ldots, \omega_n^2) \tag{19}$$

$$\Phi \equiv [\phi_1, \ldots, \phi_n] \tag{20}$$

$$\phi_i^T \boldsymbol{M} \phi_i = m \tag{21}$$

$$\phi_i^T \boldsymbol{K} \phi_i = \omega_i^2 m \tag{22}$$

and where m is the total mass, and ω_i^2 and ϕ_i are the eigenvalue and the eigenvector of the ith mode of the structure whose stiffness matrix is $\boldsymbol{K}$.

The total energy of the system is

$$E = m/2(\dot{q}^T\dot{q} + q^T\Omega q + q^T G q) \tag{23}$$

From Eqs. (17), (18), and (23), the derivative of the energy can be derived as

$$\dot{E} = \tfrac{1}{2}\Sigma \dot{s}_j e_j \tag{24}$$

where

$$e_j \equiv q^T \Phi^T \Delta \boldsymbol{K}_j \Phi q \tag{25}$$

Equation (24) indicates that the total energy varies by $e_{j1} - e_{j2}$ if the value of s_j varies from -1 to 1 and from 1 to -1 when the value of e_j is e_{j1} and e_{j2}, respectively. In other words, the total energy decreases if $e_{j1} < e_{j2}$. Therefore, when the variation range of s_j is limited as Eq. (16), an efficient strategy for vibration suppression is to change the value of s_j from 1 to -1 when e_j is at a maximum and from -1 to 1 when e_j is at a minimum. This strategy is implemented by the following logic

$$s_j = \begin{cases} 1 & \text{if } \dot{e}_j > 0 \\ -1 & \text{if } \dot{e}_j < 0 \end{cases} \tag{26}$$

When the degree of freedom of the dynamic system is one, this control logic coincides with Eq. (3). If the stepwise variation of the stiffness is not practical, the following logic can be used instead of Eq. (26):

$$s_j = \begin{cases} 1 & \text{if } \alpha \dot{e}_j \ge 1 \\ \alpha \dot{e}_j & \text{if } -1 < \alpha \dot{e}_j < 1 \\ -1 & \text{if } \alpha \dot{e}_j \le -1 \end{cases} \tag{26'}$$

where α is a constant.

When $\Delta \boldsymbol{K}_j$ is proportional to the nominal stiffness of the jth variable-stiffness structural member, Eq. (25) shows that e_j is proportional to the strain energy stored in the jth variable-stiffness member. Therefore, the control logic of Eq. (26) can be implemented by monitoring the strain energy of variable-stiffness members. Because the strain energy of each variable-stiffness member can be locally measured, this control logic is suitable for local implementation.

It is also possible to introduce weighting factor ω_i^2 for the ith mode by modifying the definition of e_j as follows:

$$e_j \equiv q^T W^T \Phi^T \Delta \boldsymbol{K}_j \Phi W q \tag{25'}$$

where

$$W \equiv \mathrm{diag}(w_1, \ldots, w_n) \tag{27}$$

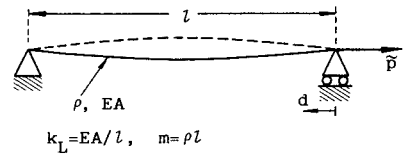

Fig. 2 Tension-stabilized string.

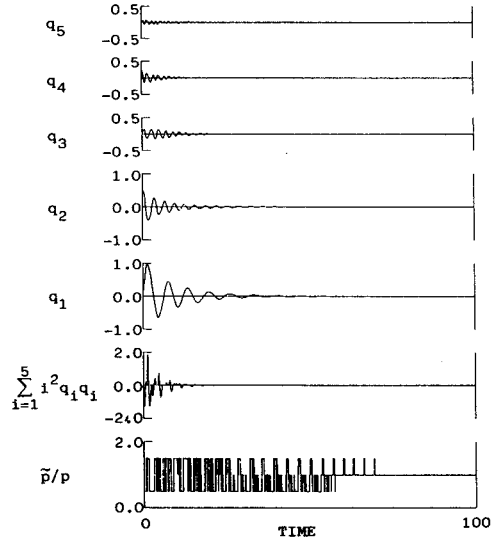

Fig. 3 Simulation result of active vibration suppression by tension control.

Active Vibration Control of a String by Tension Control

A string is the simplest and typical example of tension-stabilized structures. Therefore the investigation of the vibration suppression of the tension-stabilized string seems to suggest the characteristics of that of general tension-stabilized structures. When the external force is zero, the equation of lateral motion of the tension-controlled string shown in Fig. 2 is

$$\rho \ddot{u} - \tilde{p}(\mathrm{d}^2u/\mathrm{d}x^2) = 0 \tag{28}$$

where ρ is the mass per unit length, u the lateral displacement, $\tilde{p}$ the variable tensile force, and x the coordinate along the string. In this case, the number of variable-stiffness elements is one. The equation shows that the stiffness is proportional to the tension. Therefore, if the range of tension variation is limited as

$$(1 - \epsilon)p \le \tilde{p} \le (1 + \epsilon)p \tag{29}$$

the variation of stiffness matrix is

$$\Delta \boldsymbol{K}_1 = \epsilon \boldsymbol{K} \tag{30}$$

From the definition of Φ, it can be seen that

$$\Phi^T \Delta \boldsymbol{K}_1 \Phi = \epsilon \Phi^T \boldsymbol{K} \Phi = \epsilon m \Omega \tag{31}$$

where Ω is defined by Eq. (19) by using

$$\omega_i = \sqrt{p/\rho}\ \pi i/l \tag{32}$$

and l is the length of the string. Therefore the derivative of e_1 defined by Eq. (25) can be estimated as

$$\dot{e}_1 = 2m\epsilon q^T \Omega \dot{q} = 2m\epsilon \Sigma \omega_i^2 q_i \dot{q}_i \tag{33}$$

Because ω_i^2 is proportional to i^2, the strategy of Eq. (26) can be implemented for the string by the following control logic:

$$\tilde{p} = \begin{cases} p(1+\epsilon) \text{ (i.e., } s_1 = 1) & \text{when } \sum_i i^2 q_i \dot{q}_i \geq 0 \\ p(1-\epsilon) \text{ (i.e., } s_1 = -1) & \text{when } \sum_i i^2 q_i \dot{q}_i \leq 0 \end{cases} \tag{34}$$

When the longitudinal response of the string is fast enough compared with its lateral dynamics, the displacement of the floating end of the string d shown in Fig. 2 can be estimated as

$$d = \delta - (\tilde{p} - p)/k_L \tag{35}$$

where

$$\delta = \pi^2/(2l)\sum_i i^2 q_i^2 \tag{36}$$

and where k_L is the longitudinal stiffness of the string. Equations (35) and (36) show that $\dot{d}$ is proportional to $\sum_i i^2 q\dot{q}$ when $\tilde{p}$ is kept constant. Therefore, the control logic of Eq. (34) can be replaced by the following logic:

$$\tilde{p} = \begin{cases} p(1+\epsilon) \text{ (i.e., } s_1 = 1) & \text{when } \dot{d} \geq 0 \\ p(1-\epsilon) \text{ (i.e., } s_1 = -1) & \text{when } \dot{d} \leq 0 \end{cases} \tag{37}$$

Because d can be measured at the floating end of string, this logic can easily be implemented by a local control. This is an important advantage of this logic.

Equation (37) shows that this approach is to take out the energy of the string by using the longitudinal motion of the floating end of the string. It should also be noted that the present logic is not necessarily optimal in the sense of maximum damping per time.

To confirm the effectiveness of the present logic, a simulation was carried out based on the control logic of Eq. (37) by numerically integrating Eq. (17). Figure 3 shows an example of simulated time history of vibration suppression. Five modes are included in the mathematical model. The initial conditions are $\dot{q}_i = 1$ for $i = 1$, 3, and 5; $q_i = 1/\omega_i$ for $i = 2$ and 4; and all other q_i and $\dot{q}_i$ are zero. Other parameter values are $\omega_1 = 1$ and $\epsilon = 0.5$. In the simulation, a dead band is introduced in the logic of Eq. (37) in order to avoid excessive chattering by setting the tension as $\tilde{p} = p$ when

$$|\Sigma i^2 q_i \dot{q}_i| < 10^{-5} \tag{38}$$

The figure shows that the vibration of all of the modes is suppressed, indicating the effectiveness of the approach. Because of the dead band, the control system ceases to vary the tension when the vibration is suppressed enough.

In an actual situation, some time lag may be inevitable in the controller. Therefore, to investigate its effect, a time lag is introduced in the simulation. Figure 4 shows an example of the results, where the initial condition is the same as that of Fig. 3. The time lag is 0.135, which is only 2.1% of a cycle period of the first mode. The figure shows that the system is unstable. The mathematical model that is used in the simulation has only five modes. However, if the mathematical model includes higher modes with a nonzero initial condition, a smaller time lag causes instability. For example, a mathematical model including eight modes is unstabilized by a time lag of 0.0825, which is 1.3% of the cycle of the first mode. These examples indicate that we have to be careful when some time lag is inevitable. This possibility of instability is an annoying disadvantage of the active control. The identification of the optimal value of ϵ is still left for the future works.

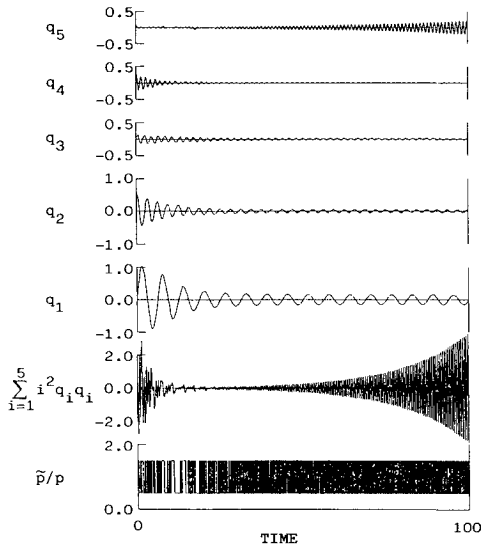

Fig. 4 Example of active tension control with a time lag.

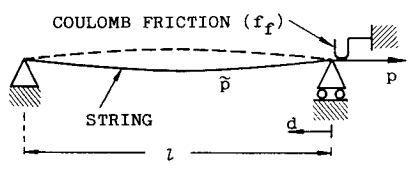

Fig. 5 Tension-stabilized string with dry friction at the floating end.

Passive Vibration Suppression of a String

To investigate if the tension control discussed in the preceding section can be implemented by a passive device, let us introduce a dry frictional device at the floating end of the string as shown in Fig. 5, where f_f is the frictional force and p the constant tension. Then it can be seen that, when δ is in the range of

$$-f_f \leq (\delta - d)k_L \leq f_f \tag{39}$$

no slip occurs, and the tension in the string is

$$\tilde{p} = p + (\delta - d)k_L \tag{40}$$

When δ exceeds the limit of Eq. (39), the frictional surface slips. If $\dot{\delta}$ is positive, the displacement and tension become

$$d = \delta - f_f/k_L \tag{41}$$

$$\tilde{p} = p + f_f \tag{42}$$

and if $\dot{\delta}$ is negative, they are

$$d = \delta + f_f/k_L \tag{43}$$

$$\tilde{p} = p - f_f \tag{44}$$

Therefore, when the value of k_L is so large that the second terms on the right-hand side of Eqs. (41) and (43) are negligible compared with the first terms, respectively, the control logic of Eq. (37) can be approximately implemented by the frictional element, i.e., by a passive device. When the amplitude of vibration is very large, the second terms can be negligible because the first terms become large, and the situation becomes the same. Because the passively damped systems are always stable and require no energy, this approach in these situations is very attractive.

To investigate the characteristics of a passively controlled system whose k_L and vibration amplitude are not so large, the damping characteristics of a single mode are studied first. Let us consider a half-cycle of free decay vibration of mode i, in which the modal displacement q_i starts from zero, goes up to the maximum value a, and again goes down to zero. Figure 6 shows the locus of state point in the δ-$\tilde{p}$ plane for this half-cycle. The amplitude of vibration is assumed to be so large that

the frictional slip occurs. Because the initial condition of this half-cycle is the final condition of the preceding half-cycle, the initial value of $\tilde{p}$ is $p - f_f$. As δ increases due to the increment of q_i, $\tilde{p}$ linearly increases in the initial phase. When the value of $\tilde{p}$ becomes $\tilde{p} = p + f_f$ at the point A of Fig. 6, the frictional slip occurs. The value of δ is $2f_f/k_L$ at this moment. When the modal displacement is at the maximum, the value of δ becomes

$$\delta_a = \pi^2 i^2 a^2/(2l) \tag{45}$$

Therefore, the length of frictional slip is

$$d_a = \delta_a - 2f_f/k_L \tag{46}$$

When the modal displacement starts to decrease, the tension $\tilde{p}$ starts to decrease. At the moment when $\tilde{p} = p - f_f$, the slip starts again, and $\tilde{p}$ remains at $p - f_f$. The length of slip in the return process is same as Eq. (46).

The initial kinematic energy is identical with the sum of the increment in the strain energy of the string and the work done by the displacement of the floating end in the initial quarter cycle. Because the displacement of the floating end is d_a, this sum, i.e., the initial kinematic energy can be obtained as follows from the figure:

$$E_I = \delta_a(p + f_f) - 2f_f^2/k_L \tag{47}$$

The dissipated energy in a half-cycle is the area inside the loop drawn by the state point in Fig. 6, which can be obtained as

$$E_D = \begin{cases} 2[\delta_a - 2(f_f/k_L)]f_f & \text{if } 2f_f/k_L \le \delta_a \\ 0 & \text{if } 2f_f/k_L \ge \delta_a \end{cases} \tag{48}$$

Therefore, the energy reduces by the factor of

$$r_h^2 = \begin{cases} \dfrac{1 - (f_f/p) + 2(f_f/p)^2[p/(k_L\delta_a)]}{1 + (f_f/p) - 2(f_f/p)^2[p/(k_L\delta_a)]} & \text{if } 2f_f/k_L \le \delta_a \\ 1 & \text{if } 2f_f/k_L \ge \delta_a \end{cases} \tag{49}$$

per half-cycle. From Eq. (49), the equivalent damping ratio defined by Eq. (9) is obtained as Fig. 7 by calculating the half-cycle duration T_h with numerical integration of the equation of motion.

The figure shows that the damping ratio is larger than 0.2 when $0.7 \le f_f/p \le 0.9$ and $7 \le k_L\delta_a/p$. If the initial condition of free vibration is in this area, the vibration damps relatively rapidly at the beginning. However, when it damps and the value of $k_L\delta_a/p$ decreases to less than 10, the damping ratio decreases. Generally, the vibration cannot damp beyond the line

$$f_f/p = 0.5k_L\delta_a/p \tag{50}$$

This is because the frictional slip at the end of string stops. From Fig. 7, we can design the system such that this passive damping becomes effective when the vibration amplitude exceeds an allowable limit. For example, the value of $k_L\delta_a/p$ has to be larger than approximately 5 to make the damping ratio

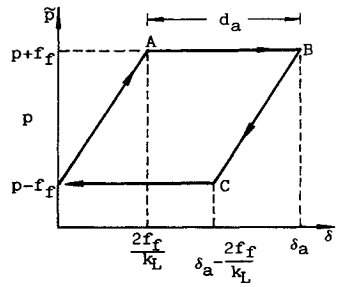

Fig. 6 Half-cycle locus of state point in δ-$\tilde{p}$ plane.

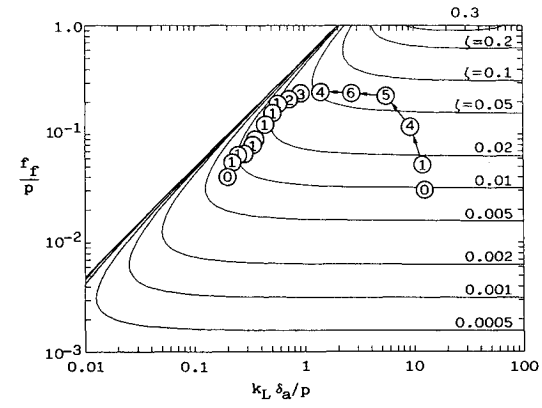

Fig. 7 Contour map of damping ratio ζ.

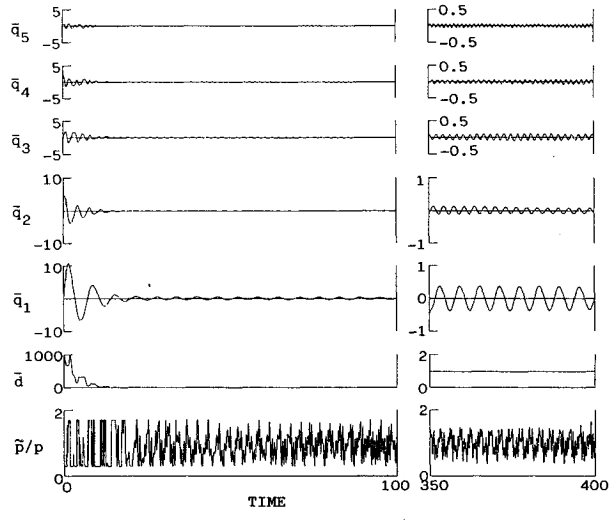

Fig. 8 Transient time history of a string with dry friction (large initial value, $f_f/p = 0.8$).

larger than 0.2. As a result, from Eq. (45), the longitudinal stiffness has to satisfy the following condition to suppress the vibration to the allowable level keeping this damping ratio of 0.2:

$$k_L \ge 10pl/(\pi i a_s)^2 \tag{51}$$

where a_s is the allowable amplitude of vibration. When Eq. (51) cannot be satisfied, the figure indicates that the maximum damping rate is obtained for the given value of $k_L\delta_a/p$ when

$$f_f/p \simeq 1/4\, k_L\delta_a/p \tag{52}$$

Therefore, to keep this damping rate until the vibration is suppressed to the allowable level, the frictional force should be adjusted as

$$f_f \simeq \frac{k_L(\pi i a_s)^2}{8l} \tag{53}$$

Unfortunately, the damping ratio decreases when the value of f_f is small, i.e., when the values of k_L and a_s are small.

To investigate the cases of the MDOF system, the lateral vibration of a string is numerically simulated. The value of ω_1 is unity, and five modes are included in the mathematical model. Figures 8–10 show the results, where

$$\bar{q}_i \equiv q_i\sqrt{k_L/(lp)} \tag{54}$$

$$\bar{d} \equiv dk_L/p \tag{55}$$

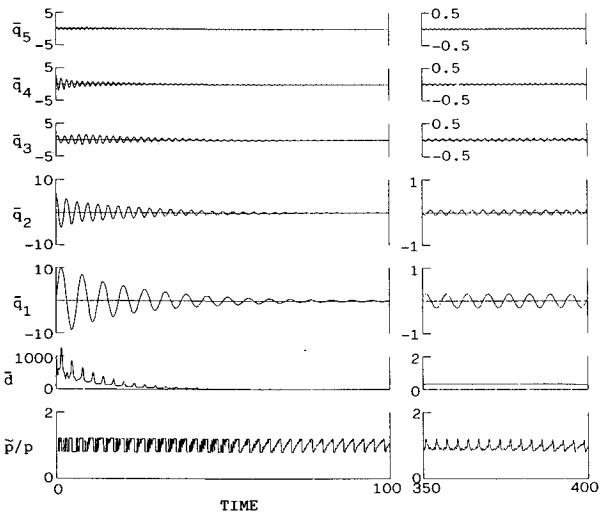

Fig. 9 Transient time history of a string with dry friction (large initial value, $f_f/p = 0.2$).

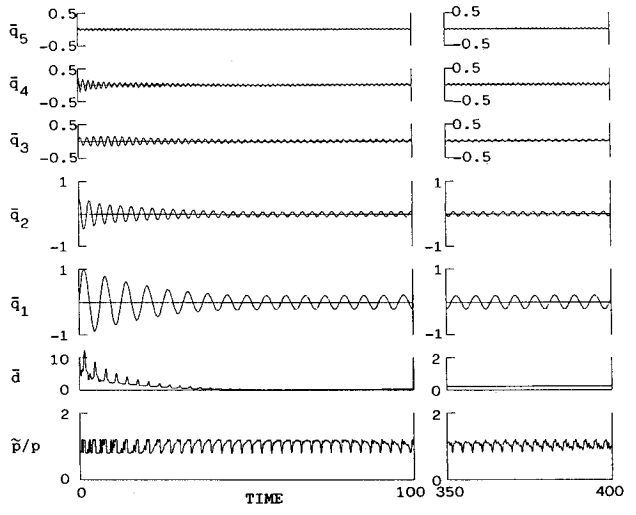

Fig. 10 Transient time history of a string with dry friction (small initial value, $f_f/p = 0.2$).

The nonzero initial values of Figs. 8 and 9 are $\dot{\bar{q}} = 10$ for $i = 1$, 3, and 5; and $\bar{q}_i = 10/\omega_i$ for $i = 2$ and 4. In Fig. 10, they are $\dot{\bar{q}}_i = 1$ for $i = 1$, 3, and 5; and $\bar{q}_i = 1/\omega_i$ for $i = 2$ and 4. The values of f_f/p are 0.8 in Fig. 8 and 0.2 in Figs. 9 and 10. It should be noted that some ordinate scales for the region of $t > 350$ are different from the others. The figures show that the vibration of all of the modes damps rapidly when the amplitude of vibration is large enough. But when the amplitude is small or has been reduced to a low level, the frictional slip stops. As a result, the vibration does not damp any more, and residual vibration remains. When the value of f_f/p is large (Fig. 8), the initial damping rate is high, but larger residual vibration remains (compared with Fig. 9). After the stop of the frictional slip, Eq. (39) is held, and the displacement of the floating end d becomes constant. In such a situation, we can see from Eq. (39) that

$$\Delta\delta k_L \simeq 2f_f \tag{56}$$

where $\Delta\delta$ is the difference between the maximum and minimum values of δ in the residual vibration. In addition, $\Delta\delta$ can be roughly estimated from Eq. (36) as

$$\Delta\delta \simeq \pi^2 \sum_i i^2 a_{ir}^2/(2l) \tag{57}$$

where a_{ir} is the amplitude of the ith mode residual vibration. Therefore, the amplitude of residual vibration can be roughly estimated as

$$\sum_i i^2 a_{ir}^2 \simeq 4f_f l/(k_L \pi^2) \tag{58}$$

The simulation results indicate that this is roughly true. The comparison of Fig. 9 with Fig. 10 shows that the amplitude of residual vibration is almost independent from the initial value of vibration. In general, the damping characteristics of a passively damped MDOF string are similar to the case of an SDOF.

Semiactive Vibration Suppression

As has been mentioned in the preceding section, the damping with dry friction has the disadvantage of residual vibration. The possibility of the variation of the frictional coefficient due to the variation of the characteristics of frictional surface is also a disadvantage. A possible approach to eliminate these disadvantages is to optimally vary the frictional force according to the state of vibration. Let us investigate the case of an SDOF system first. As has been mentioned, Fig. 7 shows that the damping ratio is larger than 0.2 in the range of $k_L\delta_a/p > 7$ when $f_f/p \simeq 0.8$. Because this damping ratio is not so bad, let us control the frictional force to be $0.8p$ in this area. When the amplitude of vibration is further reduced however, the damping rate decreases, and finally it becomes zero before the vibration damps out completely. In the cases where $k_L\delta_a/p < 3$, the maximum damping ratio is obtained when Eq. (52) is satisfied. Therefore, let us control the frictional force as Eq. (52) in this case. Because of Eq. (46) and $f_f = \Delta\tilde{p}/2$, Eq. (52) is equivalent to

$$\Delta\tilde{p} \simeq d_a k_L \tag{59}$$

where $\Delta\tilde{p}$ is the variation of $\tilde{p}$ (i.e., the difference between the maximum and minimum values) during the half-cycle. Since we can easily measure the length of slip d_a and the variation of tension $\Delta\tilde{p}$ at the floating end of the string, a convenient implementation of the aforementioned approach is to

$$\begin{aligned} &\text{increase } f_f \text{ if } \Delta\tilde{p} < d_a k_L \text{ and } \tfrac{1}{2}\Delta\tilde{p} < 0.8p \\ &\text{decrease } f_f \text{ if } \Delta\tilde{p} > d_a k_L \text{ or } \tfrac{1}{2}\Delta\tilde{p} > 0.8p \end{aligned} \tag{60}$$

In the case of MDOF, the system has many modes with different frequencies. Therefore, $\Delta\tilde{p}$ and d_a are not defined clearly, and, instead of them, we have to introduce similar indexes which represent the amounts of variations of $\tilde{p}$ and d. The difference between the maximum and minimum values in the near past can be such indexes. Figure 11 shows a possible algorithm to estimate such an index σ_α for an arbitrary variable α, where τ_f is a time constant for decay. The algorithm is a combination of peak holders and decay operators. Then an implementation of the present semiactive vibration control for MDOF system is to control f_f such that

$$\dot{f}_f/p = [(\sigma_d/\sigma_p) - \beta]/\tau_c \tag{61}$$

with a constraint

$$f_f/p \le 0.8 \tag{62}$$

where σ_d and σ_p are the indexes obtained by the algorithm in Fig. 11 for dk_L and $\tilde{p}$, respectively, β is the target value for σ_d/σ_p, and τ_c is a time constant for control.

To investigate the effectiveness of the approach, a numerical simulation is carried out. Figure 12 shows an example of time histories where the initial conditions are the same as those in Figs. 8 and 9. The parameter values for the control logic are $\beta = 1$, $\tau_f = 2$, and $\tau_c = 20$. In the figure, some ordinate scales in the region of $t > 350$ are different from the others. The figure shows that the value of f_f is at the maximum value (i.e., $0.8p$) and the damping rate is high when the amplitude of

vibration is large. When the amplitude of vibration is decreased, the value of σ_d decreases to a lower level than the value of σ_p, showing too short slip. Then the value of f_f is decreased by the control logic, and the values of σ_d and σ_p are controlled to be almost identical with each other. The comparison of the figure with Figs. 8 and 9 indicates the advantage of the semiactive control. In Fig. 12, the damping rate in the initial phase is as large as Fig. 8, and still the vibration continues to damp when it has damped to a smaller level than the amplitude of final phase of Fig. 9 whose initial damping is slow. However, even in the semiactively controlled case, the damping rate in the final phase is small compared with that of initial phase where the amplitude of vibration is large.

This control is a semiactive control, which does not directly control the structure. In this approach, the control speed may be slow compared with the period of vibration. It should be noted that when the control logic is improper, the damping becomes slow at worst. But it never becomes unstable, unlike the usual active control. Therefore, the control system can be very simple. An anxiety in using the dry friction is the possible variation of frictional coefficient. Even when it varies, this control system will adjust the normal force. Therefore, this strategy seems to overcome the disadvantages of the active and passive controls while still keeping the advantages by introducing a primitive control system. It should also be noted that this control logic can easily be implemented by a local control because it uses only the signals of d and $\tilde{p}$. This is an important advantage, especially for the flimsy tension-stabilized structures, because it is difficult to mount massive actuators and sensors on them.

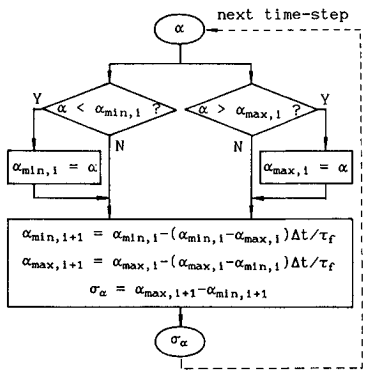

Fig. 11 Algorithm to obtain an index σ_α that represents the variation of signal α.

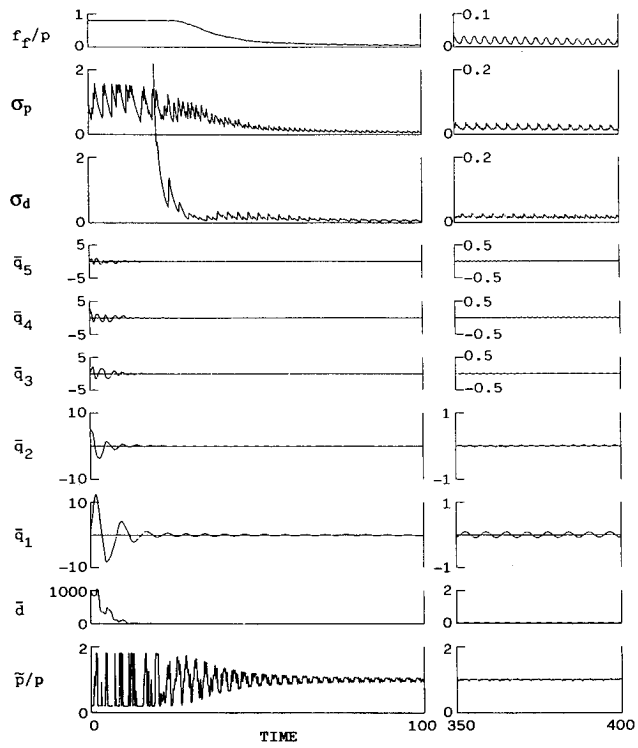

Fig. 12 Result of the simulation of semiactive vibration suppression of a string.

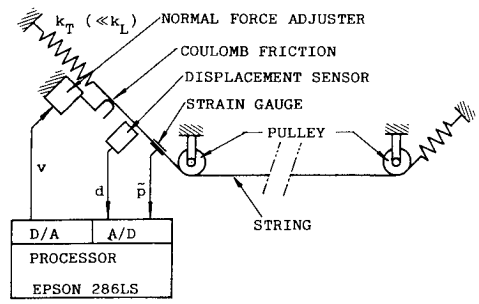

Fig. 13 Diagram of experimental setup for semiactive vibration suppression of a steel tape.

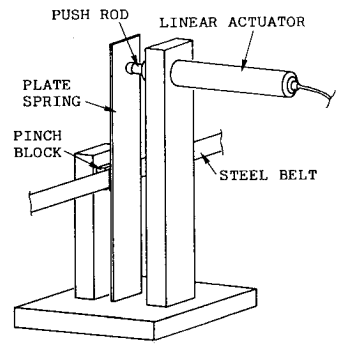

Fig. 14 Friction adjust device.

Semiactive Vibration Suppression Experiment

To confirm the effectiveness and reality of the present semiactive vibration control, an experiment on lateral vibration suppression of a steel tape was carried out. Figure 13 schematically shows the diagram of the experimental setup. The steel tape is 8 mm in width, 0.1 mm in thickness, and 2 m in length (i.e., distance between the pulleys). The longitudinal stiffness k_L is 14 N/mm when the constant tension $p = 3.2$ N is given by the soft spring k_T. At the center of the tape, a 140-g mass is attached to decrease the frequency. Lower frequency is preferable to reduce the effect of air damping and to control by using a slow processor.

The frictional force is controlled by varying the normal force on the frictional surface by using the device shown in Fig. 14. When the electromagnetic linear actuator is driven forward, the normal force for the friction increases. When it is driven backward, the normal force decreases.

In this experiment, more simple control logic than Fig. 12 is applied. The longitudinal displacement d measured by the eddy current noncontact displacement sensor and the tensile force $\tilde{p}$ measured by the strain gauge are monitored for a duration τ that is slightly longer than a cycle period of the lowest frequency. At each end of the duration, the variations (i.e., the difference between the maximum and minimum values) of each signal during the duration Δd and $\Delta\tilde{p}$ are calculated, respectively. Subsequently, the values of these two variations are compared, and the linear actuator of Fig. 14 is driven according to Table 1, which lists the drive direction and drive duration for various ranges of $\Delta d k_L/\Delta\tilde{p}$. The time constant τ_d in the table is set at 5 ms in the experiment.

In the experiment, a certain displacement is given to the center mass, and it is released. Figure 15 shows the time

Table 1 Control logic used in the experiment (duration and direction of drive)

$\Delta dk_L/\Delta\tilde{p}$	0	1/20	1/10	1/5	2/5	4/5	5/4	5/2	5	10	20	∞
Duration	$16\tau_d$	$10\tau_d$	$4\tau_d$	$2\tau_d$	τ_d	0	τ_d	$2\tau_d$	$4\tau_d$	$10\tau_d$	$16\tau_d$	
Direction	Backward					No drive	Forward					

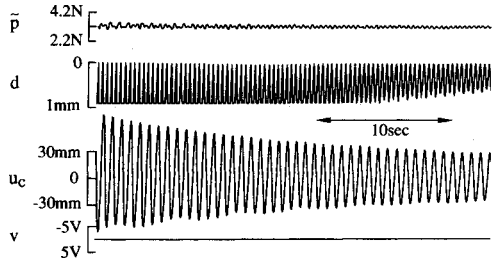

Fig. 15 Free vibration decay of steel tape without friction.

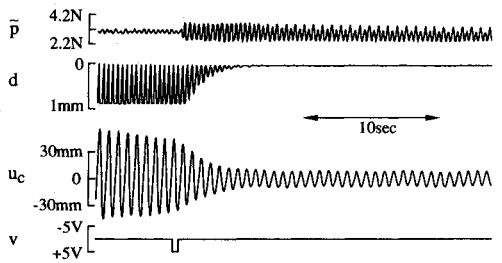

Fig. 16 Vibration decay of steel tape with constant friction.

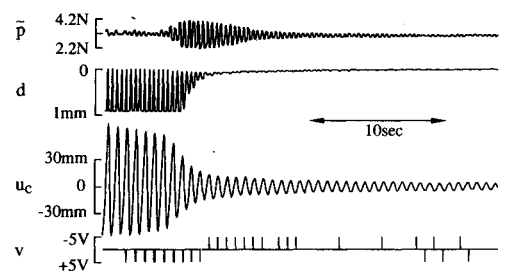

Fig. 17 Vibration decay of semiactively controlled steel tape.

history of u_c, d, and $\tilde{p}$ for the case of no friction, where u_c is the lateral displacement of the center mass measured by an optical displacement sensor. Although no frictional force is applied at the device shown in Fig. 14, vibration damps slowly due to the air damping, etc. The damping is relatively large when the amplitude of vibration is large. Because the spring constant k_T is not zero, $\tilde{p}$ varies slightly. Although the amplitude is large, measured d is saturated.

Figure 16 shows the case where a constant friction is given. Variable v denotes the drive signal for the friction adjust device. The figure shows relatively large damping when the amplitude is large. But the damping decreases extremely when the amplitude has been decreased to a low level.

Figure 17 shows the case where the present semiactive control is activated. When the control is activated, the processor senses that Δd is too large compared with $\Delta\tilde{p}$ and drives the actuator forward several times. When the frictional force becomes large, the vibration damps more rapidly than the initial phase of Fig. 16. When the vibration is damped to a lower level, the processor senses that Δd is too small, and it drives the actuator rearward several times, adjusting the friction. Although the damping rate decreases as expected from Fig. 7 when the amplitude is decreased, the vibration damps to a much smaller amplitude sooner than in Fig. 16.

From the time histories of u_c and $\tilde{p}$ of Fig. 17, the values of ζ, $k_L\delta_a/p$, and f_f/p are estimated for each cycle and plotted in Fig. 7. The numbers in the small circle are the percent values of ζ. Although the frictional force is increased only slowly because of the limitation of hardware, frictional force is controlled such that Eq. (52) is roughly satisfied enough later. The figure shows fair coincidence of the experimental and calculated values of ζ.

It should be noted that this semiactive control is very primitive, and precise information about the system is not required. In this experiment, even the quantitative relation between the actuator stroke and the frictional force is not known. Still, the system works well, demonstrating the robustness.

Concluding Remarks

An optimal on-off control logic for active vibration suppression of variable-stiffness SDOF systems has been derived. For an MDOF system with multiple variable-stiffness elements, a control logic has been proposed. This logic has been applied to a tension-controlled string and modified into a convenient form for the local implementation. Its effectiveness has been demonstrated by a numerical simulation.

It has been shown that the aforementioned control logic can be implemented by a passive device by using dry friction when the longitudinal stiffness of the string is high. The performance of the passive system with low stiffness has also been investigated. It has been shown that the damping rate decreases when the amplitude of vibration is decreased and that the vibration does not damp beyond a certain level. A guideline for the design of this passive damping system has also been proposed.

To overcome the disadvantages of the passive system, a semiactive vibration suppression approach has been proposed. A numerical simulation and an experiment of vibration suppression of a string has shown the effectiveness of the proposed semiactive approach, even though it is very primitive.

The approaches investigated in this paper seem to be most suitably applicable to the tension-stabilized structures that are too flimsy to support usual massive vibration suppression devices, because the devices for the present approaches can be incorporated into the tension control devices which are almost inevitable for the large-scale tension-stabilized structures. Although the practicality of the present approaches depends on the development of practical devices, piezoelectric materials and the Ti-Ni shape-memory alloy suggest the possibility of their realizations.

References

[1]Balas, M. J., "Trends in Large Space Structure Control Theory: Fondest Hopes, Wildest Dreams," *IEEE Transactions on Automatic Control,* Vol. AC-27, No. 3, 1982, pp. 522–535.

[2]Chen, J.-C., "Response of Large Space Structures with Stiffness Control," *Journal of Spacecraft and Rockets,* Vol. 21, No. 5, 1984, pp. 463–467.

[3]Fanson, J. L., Chen, J.-C., and Caughey, T. K., "Stiffness Control of Large Space Structures," *Proceedings of the Workshop on Identification and Control,* Jet Propulsion Lab., JPL Publication 85-29, Pasadena, CA, April 1985, pp. 351–364.

[4]Sekine, K., "Vibration Control of Membrane by Tension Variation," Master's Thesis, Univ. of Tokyo, Tokyo, Japan, 1986 (in Japanese).

[5]Onoda, J., Endo, T., Tamaoki, H., and Watanabe, N., "Vibration Suppression by Variable-Stiffness Members," *AIAA Journal,* Vol. 29, No. 6, 1991, pp. 977–983.